20

Virus diagnostics Using Fabry-Perot Interference Films of Macroporous Silicon

© K.A. Gonchar[1], N.Yu. Saushkin[2], I.I. Tsiniaikin[1], A.A. Eliseev[2,3], A.S. Gambaryan[4], J.V. Samsonova[2], L.A. Osminkina[1]¶

[1] Department of Physics, Lomonosov Moscow State University,
119991 Moscow, Russia
[2] Department of Chemistry, Lomonosov Moscow State University,
119991 Moscow, Russia
[3] Department of Material Science, Lomonosov Moscow State University,
119991 Moscow, Russia
[4] Chumakov Federal Scientific Center for Research and Development of Immunobiological Drugs
of the Russian Academy of Sciences,
108819 Moscow, Russia

e-mail: osminkina@physics.msu.ru

Received April 28, 2023
Revised July 31, 2023
Accepted September 28, 2023

In this paper, the possibility of detecting viruses, specifically influenza A virus, based on changes in the spectra of total reflection from macroporous silicon (macro-pSi) films, is demonstrated for the first time. Macro-pSi films with a pore diameter of about 100 nm were produced by electrochemical etching of crystalline silicon substrates. The porosity of the macro-pSi, calculated using the Bruggeman effective medium model, was 75%. Electron microscopy showed that such highly porous films adsorb of 50−100 nm in size viruses on their surface and inside the pores, but the efficiency of adsorption significantly increases when the surface of the nanostructures is functionalized with monoclonal antibodies, providing specific binding of viruses. The reflection spectra of macro-pSi films demonstrate a series of interference fringes, the intensity of which dramatically changes upon virus adsorption. The results obtained demonstrate the possibility of a simple and effective optical method for virus diagnostics using Fabry-Perot interference in macro-pSi films.

Keywords: Porous silicon, interference, sensor, antibody, virus.

DOI: 10.21883/0000000000

1. Introduction

Optical biosensorics has considerable advantages over other analytical techniques, offering fine sensitivity, ease of use, reproducibility, and reliability. Interferometry, surface plasmon resonance, diffraction gratings of photonic crystals, converters based on optical waveguides, ellipsometry, etc., may be used for signal conversion in optical sensors [1].

Thin porous silicon (pSi) films produced by electrochemical etching of single-crystalline silicon have an enormous surface area and are now used widely in the design of various optical sensors [2]. Porous silicon is commonly graded in accordance with IUPAC (International Union of Pure and Applied Chemistry) criteria with the pore size specifying the type of a porous material: micro-pSi (pores ≤ 2 nm in diameter), meso-pSi (pores 2−50 nm in diameter), or macro-pSi (pores ≥ 50 nm in diameter) [3]. The signal transmission mechanism may rely on such important pSi parameters as the sensitivity of its photoluminescence properties to the surface composition [4] (i.e., the variation of lifetime and intensity of photoluminescence induced by the adsorption of chemical [4,5] or biological [6] molecules). It has been demonstrated recently that porous silicon nanowires may be used as a sensing element of an optical oxygen sensor [7].

However, the most common optical sensors are designed around the interference of light in thin pSi films of various morphology [8]. The operation of such sensors relies on the fact that an interference pattern of Fabry−Pérot fringes governed by the effective optical film thickness [8,9] forms when white light incident on thin pSi films is reflected from the medium–pSi and pSi–crystalline silicon (c-Si) interfaces. The variation of the effective refraction index of a pSi layer after adsorption of biological molecules and cells is manifested as a shift of interference fringes and/or a change in their intensity [8–12]. The capacity to isolate different analytes by virtue of the morphological characteristics of porous films is one of the major advantages of pSi over planar optical transducers. While intact cells and microorganisms do not enter pores and may be immobilized only on the surface of pSi, small-sized molecules penetrate into pSi pores [2]. The possibility of detection of biotin molecules with quantum dots, which were introduced into the pSi layer matrix, used as optical signal amplifiers has also been demonstrated [13]. It has been found that thin pSi films may serve as an optical transducer for monitoring the

reflection spectrum variations induced by binding of certain bacteria [14]. The use of oxidized pSi conjugated with antibodies for optical detection of bacteria in „direct cell capture" tests has been reported in [14,15]. In addition, non-specific binding of viruses to the surface of nanostructures (silicon nanowire arrays) has already been demonstrated, and potential practical applications of this effect in the design of non-specific optical [16] and impedance [17] sensors for diagnostics of viral diseases have been examined.

The aim of the present study was to evaluate the potential for detection of viruses (with influenza A virus serving as an example) via non-specific and specific binding to nanostructured macro-pSi Fabry–Pérot films acting as sensing elements. To that end, a method for fabrication of macroporous silicon films with an approximate pore diameter of 100 nm was developed, the morphology of synthesized nanostructures was examined, a technique for functionalization of films with monoclonal antibodies to viruses was developed, and the variation of interference spectra upon influenza A virus adsorption was analyzed.

2. Experimental procedure

2.1. Synthesis of nanostructures

Macro-pSi films were fabricated by electrochemical etching of *p*-type c-Si substrates with crystallographic orientation (100) and a resistivity of 1–5 mΩ·cm in a 1 : 3 solution of fluoric acid (HF) and ethanol (C_2H_5OH) in a Teflon cell at an etching current density of 50 mA/cm^2. The surface oxide was removed from the initial c-Si wafers prior to etching by immersing them into 5M HF. The method of sacrificial etching was used to obtain uniform macro-pSi films [18]: the first porous layer etched for 30 s was removed from the c-Si surface by immersing the substrate with a film for 2 min into a 2M NaOH solution. To complete the preparation of a macro-pSi film, the c-Si substrate was rinsed with distilled water and etched again in a 1 : 3 HF:C_2H_5OH solution for 2–3 min.

2.2. Non-specific and specific binding of influenza A virus to the surface of nanostructures

Influenza A virus (New Caledonia/20/99(H1N1)) was used. In experiments on non-specific binding of viruses to macro-pSi, the samples were incubated for 1 h in a physiological solution (PS; 0.9% solution of NaCl in water) containing 50 μg/ml of influenza A virus. The films were then rinsed three times for 1 min in a PS with 0.05% of Tween 20 and dried in a Binder drying cabinet at 37°C.

A method for functionalization of macro-pSi with monoclonal antibodies was developed for experiments on specific binding of viruses. Monoclonal antibodies to H1 hemagglutinin of influenza A virus (IA139; HyTest, Moscow), 3-aminopropyltriethoxysilane (APTES; Sigma-Aldrich), and glutardialdehyde (25%, Sigma-Aldrich) were used. Macro-pSi samples were incubated in hydrogen peroxide (33%) for 30 min, rinsed thoroughly three times with distilled water, and incubated in a 10% solution of APTES in ethanol overnight under vigorous stirring. Following cleaning of porous films with ethanol (one time) and distilled water (five times), they were incubated for 1 h in a 2.5% solution of glutardialdehyde in PS at room temperature under stirring. The samples were then rinsed thoroughly with distilled water (five times) and incubated in a 15 μg/ml solution of specific monoclonal antibodies in PS (500 μl/plate 5 × 5 mm) for 1 h at room temperature under stirring. The prepared samples were rinsed (three times in 650 μl of PS with 0.05% Tween 20/plate) and used to perform an immunochemical specific virus reaction.

In experiments on specific virus binding, macro-pSi samples functionalized with antibodies were incubated for 1 h in a PS containing 50 μg/ml of influenza A virus. The films were then rinsed three times in a PS with 0.05% of Tween 20 and dried in a Binder drying cabinet at 37°C.

In order to obtain microscopic images of the samples with adsorbed viruses, they were dried for 5 min in a Binder drying cabinet at 37°C and subjected to fixation in a 2.5% solution of glutardialdehyde in PS (1.5 h) and a series of 50, 70, 80, and 96% aqueous alcohol solutions (10 min in each).

2.3. Examination of the morphology and optical properties of samples

The structural properties of samples were examined with a Carl Zeiss Supra 40 scanning electron microscope (SEM). Total reflectance spectra of pSi in the 12000–20000 cm^{-1} spectral range were recorded with a Perkin Elmer Lambda 950 spectrometer fitted with an integrating sphere.

3. Experimental results and discussion

SEM images of a macro-pSi sample (top and side view) are presented in Fig. 1. It is evident that the pore diameter is on the order of 100 nm (see Fig. 1, *a* and the inset in Fig. 1, *b*) and the pores themselves have the form of channels with smooth walls oriented vertically in crystallographic direction [100]. The porous layer thickness is approximately equal to 2 μm (Fig. 1, *b*).

The total reflectance spectra of macro-pSi (Fig. 2) reveal Fabry–Pérot fringes associated with interference in thin films upon reflection of two rays from air–macro-pSi and macro-pSi–c-Si interfaces. The effective refraction index ($n_{\text{eff}} = 1.3$) for the initial macro-pSi sample was calculated in accordance with the following formula from [19]:

$$n_{\text{eff}} = \frac{1}{2L\Delta k}, \tag{1}$$

where L is the macro-pSi film thickness and Δk is the distance between the interference peaks in Fig. 2 (curve *1*).

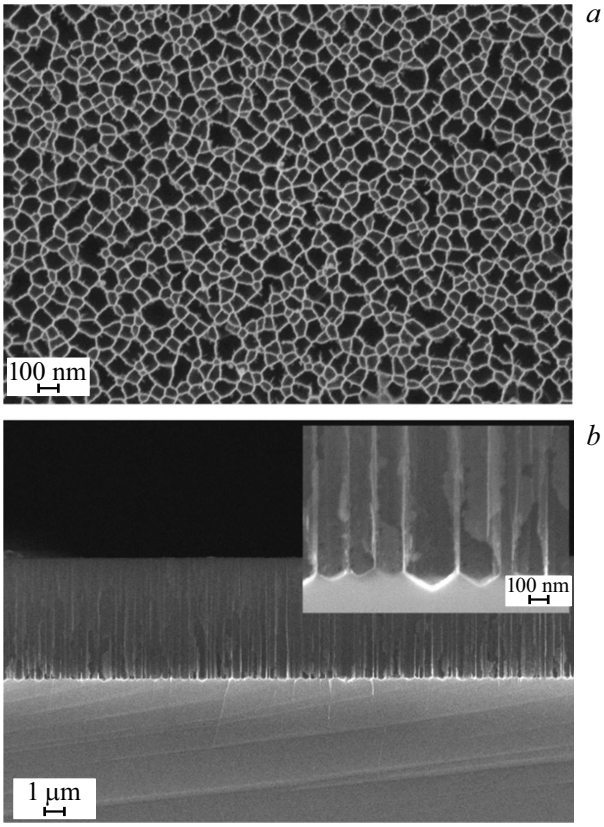

Figure 1. SEM images of a pSi sample: (*a*) top view and (*b*) side view (an enlarged fragment is shown in the inset).

Effective permittivity (ε_{eff}) of samples was calculated as

$$\varepsilon_{\text{eff}} = n_{\text{eff}}^2. \qquad (2)$$

The Bruggeman effective medium model [20] was used to calculate the porosity of samples:

$$f_{\text{air}} \frac{\varepsilon_{\text{eff}} - \varepsilon_{\text{air}}}{\varepsilon_{\text{eff}} + l(\varepsilon_{\text{air}} - \varepsilon_{\text{eff}})} + f_{\text{Si}} \frac{\varepsilon_{\text{eff}} - \varepsilon_{\text{Si}}}{\varepsilon_{\text{eff}} + l(\varepsilon_{\text{Si}} - \varepsilon_{\text{eff}})} = 0 \qquad (3)$$

where $\varepsilon_{\text{air}} = 1$ is the permittivity of air, $\varepsilon_{\text{Si}} = 11.8$ is the permittivity of silicon, $l = 0.5$ is the depolarization factor for a cylinder (pores in macro-pSi may be regarded as cylinders), f_{air} is the air fill factor (macro-pSi porosity), and f_{Si} is the silicon fill factor. Relation $f_{\text{air}} + f_{\text{Si}} = 1$ holds true in this case. The macro-pSi film porosity calculated in accordance with the presented model was 75%.

The fast Fourier transform (FFT) of the obtained interference spectra is shown in the inset of Fig. 2, where effective optical thickness ($2Ln$) of the sample and the signal amplitude are plotted on the abscissa and ordinate axes, respectively [21]. It is evident that the signal amplitude decreases slightly following non-specific virus adsorption. This may be attributed to the scattering of light off virus particles introduced into the porous macro-pSi matrix.

Figure 3 shows the total reflectance spectra of a macro-pSi film functionalized with antibodies before (*1*) and after (*2*) virus adsorption.

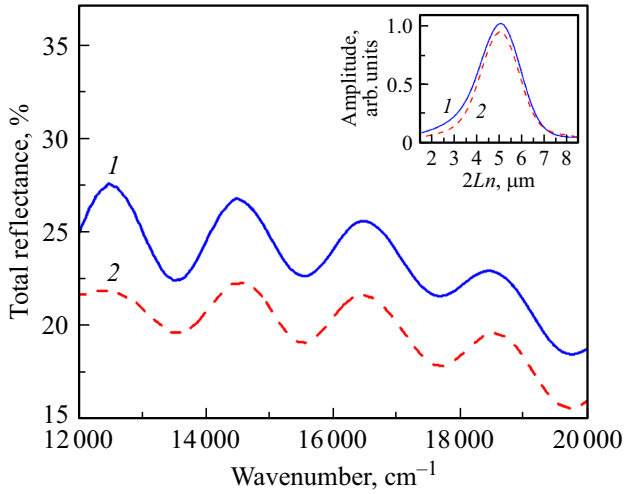

Figure 2. Total reflectance spectra of a macro-Psi film before (*1*) and after (*2*) non-specific adsorption of influenza A virus. The fast Fourier transform of interference spectra is shown in the inset.

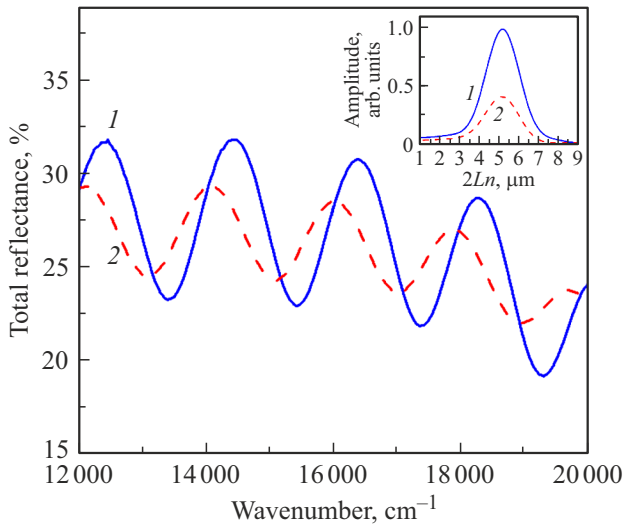

Figure 3. Total reflectance spectra of a macro-pSi sample functionalized with antibodies before (*1*) and after (*2*) adsorption of influenza A virus. The FFT of interference spectra is shown in the inset.

Note that the effective optical thickness of samples remains the same after the adsorption of viruses with non-specific and specific binding to the macro-pSi surface. This may be attributed to the fact that n_{eff} of the macro-pSi film remains unchanged following the adsorption of viruses, since the refraction indices of viruses (1.5 [22]) and the porous film are close. However, the signal amplitude in the FFT spectra of macro-pSi films functionalized with antibodies decreases by a factor of 2.2 after virus adsorption. This is likely related to the efficient interaction of viruses with the porous surface of samples coated with antibodies.

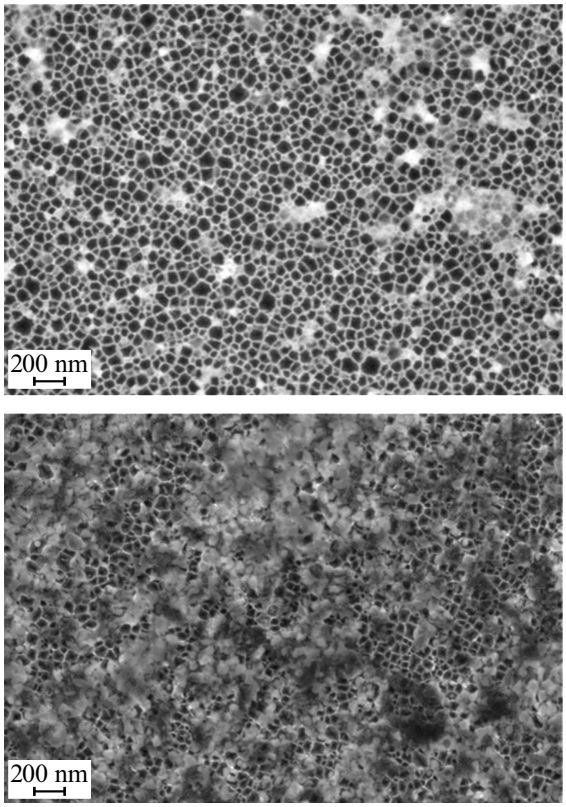

Figure 4. SEM images (top view) of macro-pSi films in experiments on non-specific (*a*) and specific (*b*) binding of influenza A virus.

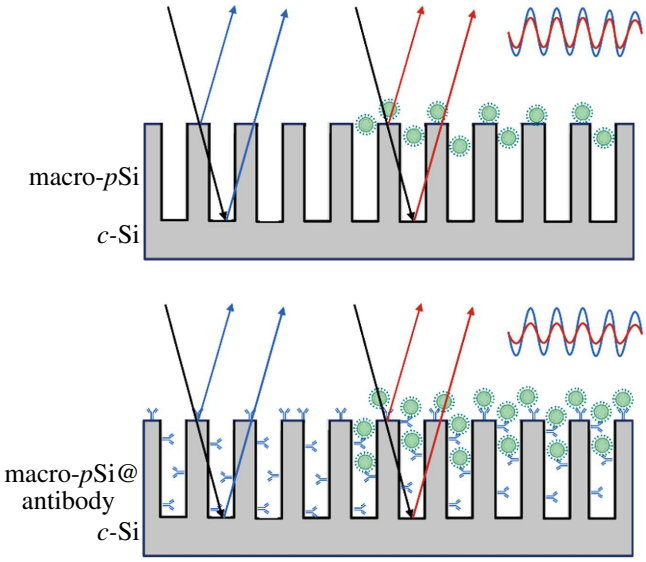

Figure 5. Schematic diagram of optical readout of sensor response as a variation of amplitude of interference spectra of macro-pSi films upon non-specific and specific binding of viruses to the surface of nanostructures.

Figure 4 shows the SEM images (top view) of macro-pSi samples in experiments on non-specific and specific binding of influenza A virus to the film surface.

In the case of non-specific binding, only a few isolated virus particles are seen on the surface and in pores of macro-pSi films; after specific binding, almost the entire film surface is covered with these particles. This is attributable to the fact that virus particles in experiments on non-specific binding interact with the surface of porous films via van der Waals forces [23], and most of them are washed away when the sample is rinsed. In the case of specific adsorption, the virus forms strong covalent bonds with antibodies on the macro-pSi surface, and only a minor fraction of its particles are removed in the course of rinsing. Figure 5 presents a schematic diagram of the above-described non-specific and specific binding of viruses to the macro-pSi surface and the mechanism of optical sensor response readout.

4. Conclusion

A method for fabrication of macroporous silicon films with a pore diameter on the order of 100 nm and a technique for functionalization of film surfaces with monoclonal antibodies to influenza A viruses were developed. It was demonstrated that a series of interference fringes (with their amplitude changing after virus adsorption) forms in the total reflectance spectra of samples. The porosity of samples calculated using the Bruggeman effective medium model was 75%. SEM images revealed that this nanostructure morphology enables efficient non-specific and specific adsorption of viruses. Non-specific binding may be supported by interactions between the developed porous surface of nanostructures and the surface of virus particles. Functionalization with monoclonal antibodies ensures tight virus binding, which is evidenced by a sharp drop in amplitude of the FFT of interference spectra of porous films. The presented sensing systems based on macroporous silicon are potentially universal in nature and may be used to construct sensors for various types of viruses.

The obtained results open up potential for macro-pSi films to be used as efficient interference optical sensors for diagnostics of viral diseases.

Acknowledgments

Equipment provided by the Training Methodical Center of Lithography and Microscopy of the Moscow State University was used in the study.

Funding

The study was supported by the Russian Science Foundation, grant No. 22-72-10062 https://rscf.ru/en/project/22-72-10062/

Conflict of interest

The authors declare that they have no conflict of interest.

References

[1] M. Nirschl, F. Reuter, J. Vörös. Biosensors, **1**(3), 70 (2011). DOI: 10.3390/bios1030070

[2] G. Shtenberg, E. Segal. *Porous silicon optical biosensors. Handbook of Porous Silicon* (Springer International Publishing, Cham, Switzerland, 2014). DOI: 10.1007/978-3-319-71381-6_87

[3] J. Rouquerol, D. Avnir, C.W. Fairbridge, D.H. Everett, J.M. Haynes, N. Pernicone, J.D.F. Ramsay, K.S.W. Sing, K.K. Unger. Pure & Appl. Chem., **66**(8), 1739 (1994). DOI: 10.1351/pac199466081739

[4] A.G. Cullis, L.T. Canham, P.D.J. Calcott. J. Appl. Phys., **82**, 909 (1997). DOI: 10.1063/1.366536

[5] E.A. Konstantinova, Y.V. Ryabchikov, L.A. Osminkina, A.S. Vorontsov, P.K. Kashkarov. Semicond., **38**(11), 1344 (2004). DOI:10.1134/1.1823072.

[6] M.J. Sailor, E.C. Wu. Adv. Funct. Mat., **19**(20), 3195 (2009). DOI: 10.1002/adfm.200900535

[7] V.A. Georgobiani, K.A. Gonchar, E.A. Zvereva, L.A. Osminkina. Phys. Stat. Sol. A, **215**(1), 1700565 (2018). DOI: 10.1002/pssa.201700565

[8] A. Jane, R. Dronov, A. Hodges, N.H. Voelcker. Trends in biotech., **27**(4), 230 (2009). DOI: 10.1016/j.tibtech.2008.12.004

[9] V.S. Lin, K. Motesharei, K.P. Dancil, M.J. Sailor, M.R. Ghadiri. Science, **278**(5339), 840 (1997). DOI:10.1126/science.278.5339.840

[10] M.B. Gongalsky, A.A. Koval, S.N. Schevchenko, K.P. Tamarov, L.A. Osminkina. J. Electr. Soc., **164**(12), B581 (2017). DOI: 10.1149/2.1821712jes

[11] N. Massad-Ivanir, G. Shtenberg, E. Segal. J. Vis. Exp., **81** (2013). DOI: 10.3791/50805

[12] N. Massad-Ivanir, G. Shtenberg, N. Raz, C. Gazenbeek, D. Budding, M.P. Bos, E. Segal. Sci. Rep., **6**, 38099 (2016). DOI: 10.1038/srep38099

[13] G. Gaur, D.S. Koktysh, S.M. Weiss. Adv. Funct. Mat., **23**(29), 3604 (2013). DOI: 10.1002/adfm.201202697

[14] N. Massad-Ivanir, Y. Mirsky, A. Nahor, E. Edrei, L.M. Bonanno-Young, N.B. Dov, A. Sa'ar, E. Segal. Analyst, **139**, 3885 (2014). DOI: 10.1039/C4AN00364K

[15] N. Massad-Ivanir, G. Shtenberg, E. Segal. Adv. Exp. Med. Biol., **733**, 37 (2012). DOI: 10.1007/978-94-007-2555-3_4

[16] K.A. Gonchar, S.N. Agafilushkina, D.V. Moiseev, I.V. Bozhev, A.A. Manykin, E.A. Kropotkina, A.S. Gambaryan, L.A. Osminkina. Mater. Res. Express, **7**, 035002 (2020). DOI: 10.1088/2053-1591/ab7719

[17] M.B. Gongalsky, U.A. Tsurikova, J.V. Samsonova, G.Z. Gvindzhiliiia, K.A. Gonchar, N.Yu. Saushkin, A.A. Kudryavtseva, E.A. Kropotkina, A.S. Gambaryan, L.A. Osminkina. Res. Mat., **6**, 100084 (2020). DOI: 10.1016/j.rinma.2020.100084

[18] J. Li, M.J. Sailor. Biosens. Bioelectron., **55**, 372 (2014). DOI: 10.1016/j.bios.2013.12.016

[19] B. Rossi. *Optics* (Addison-Wesley, Reading, MA, USA,1957).

[20] D.A.G. Bruggeman. Ann. Phys. (Leipzig), **416**(7), 636 (1935). DOI: 10.1002/andp.19354160705

[21] M.J. Sailor. *Porous Silicon in Practice: Preparation, Characterization and Applications* (Wiley-VCH Verlag GmbH & Co. KGaA, Weinheim, Germany, 2012).

[22] S.Wang, X.Shan, U.Patel, X. Huang, J. Lu, J. Li, N. Tao. PNAS, **107**, 16028 (2010). DOI: 10.1073/pnas.1005264107

[23] L.A. Osminkina, S.N. Agafilushkina, E.A. Kropotkina, N.Yu. Saushkin, I.V. Bozhev, S.S. Abramchuk, J.V. Samsonova, A.S. Gambaryan. Bioact. Mat., **7**, 39 (2022). DOI: 10.1016/j.bioactmat.2021.06.001

Translated by D.Safin